Following the molecular motion of near-resonant excited CO on Pt(111): A simulated x-ray photoelectron diffraction study based on molecular dynamics calculations

Greif, Michael ; Nagy, Tibor ; Soloviov, Maksym ; Castiglioni, Luca ; Hengsberger, Matthias ; Meuwly, Markus ; Osterwalder, Jürg

DOI: https://doi.org/10.1063/1.4922611

Following the molecular motion of near-resonant excited CO on Pt(111): A simulated x-ray photoelectron diffraction study based on molecular dynamics calculations

Michael Greif, Tibor Nagy, Maksym Soloviov, Luca Castiglioni, Matthias Hengsberger, Markus Meuwly, and Jürg Osterwalder

Citation: Structural Dynamics **2**, 035102 (2015); doi: 10.1063/1.4922611
View online: http://dx.doi.org/10.1063/1.4922611
View Table of Contents: http://scitation.aip.org/content/aca/journal/sdy/2/3?ver=pdfcov
Published by the American Crystallographic Association, Inc.

Following the molecular motion of near-resonant excited CO on Pt(111): A simulated x-ray photoelectron diffraction study based on molecular dynamics calculations

Michael Greif,[1] Tibor Nagy,[2,3] Maksym Soloviov,[2] Luca Castiglioni,[1] Matthias Hengsberger,[1] Markus Meuwly,[2] and Jürg Osterwalder[1]
[1]*Departement of Physics, University of Zürich, Winterthurerstrasse 190, CH-8057 Zürich, Switzerland*
[2]*Department of Chemistry, University of Basel, Klingelbergstrasse 80, CH-4056 Basel, Switzerland*
[3]*IMEC, RCNS, Hungarian Academy of Sciences, Magyar tudósok körútja 2, HU-1117 Budapest, Hungary*

(Received 24 February 2015; accepted 3 June 2015; published online 17 June 2015)

A THz-pump and x-ray-probe experiment is simulated where x-ray photoelectron diffraction (XPD) patterns record the coherent vibrational motion of carbon monoxide molecules adsorbed on a Pt(111) surface. Using molecular dynamics simulations, the excitation of frustrated wagging-type motion of the CO molecules by a few-cycle pulse of 2 THz radiation is calculated. From the atomic coordinates, the time-resolved XPD patterns of the C 1s core level photoelectrons are generated. Due to the direct structural information in these data provided by the forward scattering maximum along the carbon-oxygen direction, the sequence of these patterns represents the equivalent of a molecular movie. [http://dx.doi.org/10.1063/1.4922611]

I. INTRODUCTION

Pump-probe experiments have brought about the field of femtochemistry[1] where the molecular dynamics in chemical reactions is studied in real time. An ultrashort pump pulse of laser light triggers some process in a molecule, while a probe pulse of electrons or electromagnetic radiation records the transient structural changes either directly in the nuclear coordinates or indirectly via the electronic or vibrational properties of the system after a defined delay on the femtosecond time scale. Pulsed electron and x-ray diffraction have been successfully used as time-resolved direct structural probes for molecules in the gas phase.[2,3] However, many important chemical reactions can be boosted and steered by heterogeneous catalysis, where the molecules are adsorbed on a solid surface.[4,5] Surface sensitive techniques with femtosecond temporal resolution have been developed over the last two decades. Bond weakening and bond breaking processes have been followed by time-resolved non-linear optical methods[6] and by time-resolved two-photon photoemission.[7,8] More recently, the advent of x-ray free-electron lasers (XFEL) has made it possible to observe bond breaking and bond formation on surfaces via x-ray absorption and x-ray emission experiments.[9,10] On the other hand, experiments measuring the dynamics of the nuclear coordinates on surfaces directly via time-resolved diffraction methods have remained scarce,[11] which reflects the difficulty of obtaining such data on a femtosecond time scale.

Photoelectron diffraction comes up as a promising probe technique, because the photoexcitation process is on the attosecond time scale[12] and the detected photoelectrons probe only the surface region of a solid due to their short inelastic mean free paths. The kinetic energy distribution of the photoelectrons reflects the molecular orbital energies and core levels of the adsorbed molecules, while their angular distribution contains information on bond angles and distances. This is due to a diffraction effect where a photoelectron wave is produced at one particular atom

within the molecule and subsequently scattered coherently off the neighboring atoms.[13] The photoemitter can be selected by measuring the intensity distribution of the corresponding core-level spectrum.

A necessary condition for the observation of photoelectron diffraction from molecular adsorbates is that all molecules within the sampled surface area are oriented in a unique way. Orientational disorder, be it static or thermal, will reduce the diffraction contrast. This applies also to studies of structural dynamics, and therefore any pump-probe scheme using this technique requires the excitation of coherent molecular motion. Optical mechanisms for inducing vibrational coherence are well established and have permitted the study of vibrational relaxation on the femtosecond time scale by optical means, exploiting the transient changes of a macroscopic polarization.[14] Recently, the use of THz pulses, exerting a time-dependent torque on molecular dipoles, has been proposed as a trigger for coherent motion inducing a chemical reaction.[15]

Time-resolved photoelectron diffraction experiments are becoming possible with the availability of ultrashort x-ray pulses from an XFEL or from higher harmonics generation using intense laser pulses. This article presents a simulation of what one can expect from an experiment using x-ray pulses a few tens of femtoseconds long with a photon energy of 1000 eV. The simple case of a diatomic molecule bonded in an upright orientation at a metal surface will be represented by the system of CO molecules adsorbed on a Pt(111) surface. The simulated process is the near-resonant excitation of a frustrated "wagging"-type translation of the molecule by a THz pulse (see Fig. 1). The coupling of the molecular motion to the THz field is described simply by putting point charges on the carbon and oxygen atoms, and no electronic friction is considered. The resulting dynamics therefore lacks some features, most importantly the damping of the field-induced wagging motion. Nevertheless, such *toy model* calculations provide important insight into what is left in terms of x-ray photoelectron diffraction (XPD) modulations when an ensemble of molecules is coherently excited.

II. THE SYSTEM

Platinum is a well established and efficient catalyst for reactions of carbon monoxide, and as such has been of great interest to the chemical industries for a long time.[16] There have been

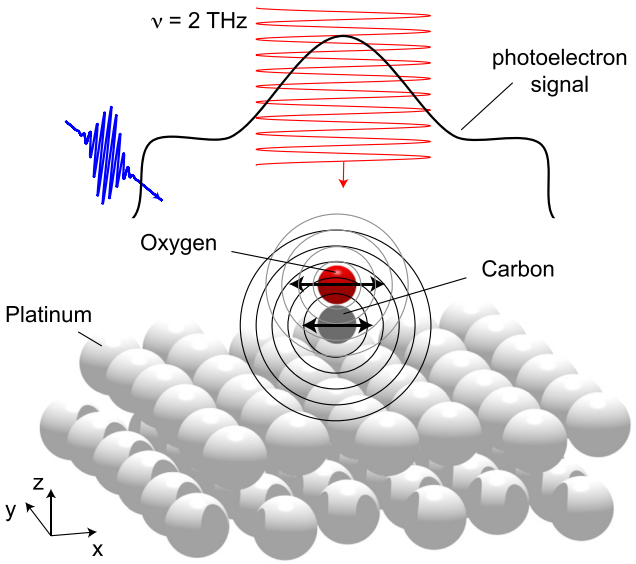

FIG. 1. Sketch of the pump-probe experiment to record time-resolved XPD data. The 2 THz pulse (red) acts as pump pulse and the CO molecule on top of the Pt(111) surface follows the field of the THz radiation (black arrows). With the (blue) x-ray pulse the molecular orientation is probed by recording an XPD pattern. The unscattered C 1s photoelectron wave is indicated by solid circles, the wave scattered off the oxygen atom by light grey circles. The solid curve above the surface illustrates the resulting C 1s intensity distribution. Note: The wavelength of the 2 THz pulse is much larger ($\lambda \approx 150\,\mu$m) than shown here.

numerous studies examining the system CO on Pt(111) with different experimental methods.[17,18] From LEED and thermal desorption experiments, the CO adsorption behavior is well known.[19–21] For coverages $\Theta < 1/6$, the molecules adsorb exclusively on energetically favored atop sites of the platinum surface. For $\Theta > 1/6$, they adsorb also on the bridge sites, until at $T = 300\,\mathrm{K}$ the coverage is saturated at $\Theta = 0.5$, where a $c(4 \times 2)$ superstructure emerges.[22] At this coverage, 50% of the molecules are adsorbed on the bridge and 50% on the atop site. With increasing coverage, the work function of the CO/Pt(111) system shows a peculiar behavior: before the coverage reaches $\Theta = 1/6$ the work function continuously decreases but rises again for higher coverages until at $\Theta = 0.5$ it has nearly the same value as the pristine metal surface. This behavior could be explained by different local dipole moments of CO at the two different adsorption sites.[19] Later calculations showed that the dipole moment of CO has indeed opposite sign when adsorbed on the bridge site as compared to the atop site.[23] It is known that the small dipole moment of CO depends on the strength of the bonding to a metal surface,[24] and a change of adsorption site could lead to the observed change of polarity.

The molecules are chemisorbed mainly by hybridization of the molecular 5σ-orbital and the sp-band of the platinum, and back-donation of metallic d-electrons into the $2\pi^*$ orbitals.[25,26] The 5σ molecular orbital is located largely on the carbon atom which is close to the surface, while the oxygen atom points away from the surface,[21] forming a linear Pt-CO equilibrium configuration at the atop site, perpendicular to the surface as shown in Fig. 2. The molecules are thus in an upright position, with wagging-type frustrated translations forming the lowest-energy nuclear degrees of freedom. This model was corroborated in a XPD study by Wesner *et al.*[27] The intensity of the C 1s core-level is enhanced along the CO bond axis due to strong forward scattering off the oxygen atom, and the corresponding peak was found to be centered along the surface normal. The width of this peak was broader than what is expected from single-scattering cluster calculations (SSC). This was explained with a wagging-type motion of the CO molecule caused by a frustrated translation. Assuming an isotropic azimuthal distribution of this wagging motion, a line shape analysis showed that the maximum tilt angle of the molecules should be less than $\theta = 10^\circ$ at room temperature.

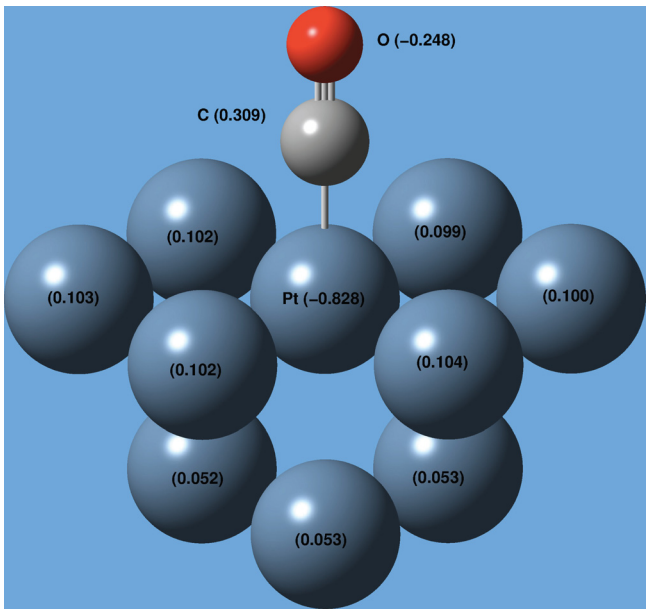

FIG. 2. Atop bonding configuration of CO on Pt(111): Mulliken charges in atomic unit (e) determined for a singlet ($S = 0$) Pt_{7-3} – CO cluster from BMK density functional theory calculations using 6-31G* and LANL2DZ basis sets (see text). Positions of carbon and oxygen atoms were optimized, while the geometry of Pt atoms was fixed as in bulk metal. The surface of the cluster where the CO binds corresponds to the (111) lattice plane.

In order to characterize the diffusion, desorption and dissociation characteristics of the molecules, the system was also examined with vibrational spectroscopy. One of the normal modes discovered in a helium scattering experiment was attributed to precisely the frustrated translational mode of the CO on Pt(111) mentioned above. The corresponding vibrational frequency at a saturated coverage was measured to be $\nu = 1.79$ THz,[28] without showing any wave vector dependence. This means that the mutual interaction between the adsorbed molecules is weak.

It was recently suggested that the wagging motion of the polar CO molecule could be enhanced by intense THz laser pulses of resonant frequency so that the molecules tilt down close enough to the surface to initiate a dissociation reaction.[15] Here, we propose and simulate an experiment in a regime where the THz pulses do not tilt the molecules entirely down to the surface, but rather lead to a coherent wagging motion of an ensemble of molecules. It is shown that the molecular motion can then be followed in real time with a time-resolved XPD experiment using a pump-probe setup. In such a measurement, a THz pulse acts as the pump pulse to excite the frustrated translational mode coherently, while a synchronized pulsed x-ray beam, e.g., from an XFEL, acts as the probe pulse with a variable delay. Selecting the C 1s core level as emitter, XPD patterns can be recorded for a sequence of time delays on the femtosecond scale between the two pulses. In these patterns, the position of the carbon-to-oxygen forward scattering peak allows to follow the orientation of the molecule on an ultrashort time scale. From such data, one can thus directly produce a molecular movie.

III. METHODS

A. Atomistic simulations

To simulate this experiment, the motion of a CO molecule on a small atomic slab representing the Pt(111) surface was calculated before, during, and after the arrival of a THz pulse, which was represented by a few-cycle periodic perturbation (*v.i.*). All molecular dynamics (MD) simulations[29,30] were carried out with the CHARMM code.[31] The system consisted of one CO molecule and a 7-layer, 6×6 Pt(111) surface with 2D-periodic boundary conditions. The interaction among the atoms and with the external electric field of the exciting THz pulse was described via a conventional force field parametrization. Different parametrizations for the non-bonded (electrostatic and van der Waals parameters) CO adsorbate were used. In one of them, only the electrostatics was retained (see Table I) but there were also simulations with standard van der Waals parameters.[31]

The interaction among the Pt atoms in the fcc lattice was described with a 12-6 Lennard-Jones potential according to Heinz *et al.*[32] with a cutoff of 12 Å. The parametrization reproduces the experimental density (with $+0.02\%$ of error), surface tension (-0.2%) as well as mechanical properties (Young modulus ($+4\%$), bulk modulus (-17%), shear modulus ($+6\%$), and the Poisson ratio ($+7\%$)) of platinum in quantitative to good qualitative agreement with

TABLE I. Force field parametrization of the system. The electric field of the THz pulse was polarized parallel to the surface, along the x-axis.

Atoms	Potential	r_0, θ_0	$q, \epsilon_0, k_r, k_\theta$
C	Electrostatic: $-q \cdot E_x(t) \cdot x$	—	$+0.5e$
O	Electrostatic: $-q \cdot E_x(t) \cdot x$	—	$-0.5e$
Pt $\cdots$ Pt	L-J: $\epsilon_0\left[\left(\frac{r_0}{r}\right)^{12} - 2\left(\frac{r_0}{r}\right)^{6}\right]$	2.845 Å	$7.8\,\frac{\text{kcal}}{\text{mol}}$
Pt-C	Stretch: $\frac{k_r}{2}(r - r_0)^2$	1.95 Å	$565\,\frac{\text{kcal}}{\text{mol Å}^2}$
C-O	Stretch: $\frac{k_r}{2}(r - r_0)^2$	1.15 Å	$2364\,\frac{\text{kcal}}{\text{mol Å}^2}$
Pt-C-O	Bend: $\frac{k_\theta}{2}(\theta - \theta_0)^2$	180°	$64.3\,\frac{\text{kcal}}{\text{mol(deg)}^2}$
Pt $\cdots$ Pt-C	Bend: $\frac{k_\theta}{2}(\theta - \theta_0)^2$	90°	$27.54\,\frac{\text{kcal}}{\text{mol(deg)}^2}$

experiments at ambient conditions. The same parametrization was used for all Pt atoms regardless of their distance from the surface or interaction with the CO molecule.

The interactions between the three covalently bonded central atoms (Pt-C-O) were described by harmonic bond (Pt-C, C-O) and angle (Pt-Pt-C, Pt-C-O) potentials. Equilibrium bond lengths were taken from the literature, and force constants were tuned such as to match the experimentally determined frequencies.[21] For determining the point charges on the atoms, density functional theory (DFT) calculations were carried out for a Pt_{7-3}–CO cluster consisting of 7 Pt atoms in the top layer and 3 Pt atoms in the bottom layer (Fig. 2), using Gaussian09.[33] The BMK (Boese-Martin for Kinetics) hyper-GGA functional[34] was used, which was proven to be the most reliable for small Pt_x–CO clusters for predicting binding-site preference.35 Basis sets 6–31G* and LANL2DZ (core potential + basis) were used for CO and Pt atoms, respectively. The lowest energy singlet state ($S = 0$), representing the ground state, was investigated in our calculations.

First, the positions of the carbon and oxygen atoms were optimized while the Pt atoms were kept fixed at distances corresponding to bulk fcc Pt. The DFT calculation suggests Mulliken charges[36] of $+0.31e$ and $-0.25e$ for C and O atoms, respectively (see Fig. 2). A mirror dipole of CO can be observed in the Pt_{7-3} cluster with significant atomic charges. As the interaction with the external electric field is shielded in the bulk metal, zero charge was assigned to all Pt atoms in the slab model. Furthermore, as an approximation, atomic point charges $+0.5$ and -0.5 were assigned to the C and O atoms, respectively. Predicting the dipole moment even for a free CO molecule in vacuum is a challenging problem in quantum chemistry. The performance of various methods varies considerably with the level and precise nature of theory and depends sensitively on the basis set.[37] The task for accurate calculations is even more formidable when other atoms, especially transition metal atoms, are bonded to CO. Depending on the chemical environment, adsorption site, and occupation of neighbouring adsorption sites, different charge distributions on the CO adsorbate have been found previously.[23]

The time evolution of the system was followed from atomistic simulations which were carried out as follows. First, the system was heated and equilibrated at $T = 300\,\mathrm{K}$, followed by an equilibrium (*NVT*) dynamics at constant volume and temperature. Excitation by the electric field was mimicked by a cosine pulse of frequency $\nu = 2$ THz with a pulse duration of 5 ps, covering 10 optical cycles, with a polarization parallel to the surface (see Fig. 1). The field amplitude of 6×10^8 V/m induces motion parallel to the surface (hindered translation) by coupling to the point charges on the polar CO molecule. After the pulse was switched off (5 ps later), the system was allowed to propagate freely.

B. Simulations of diffraction maps

From the MD calculations performed with the CO molecule sitting on a 7-layer Pt slab, the coordinates of atoms within a smaller cluster consisting of two layers of Pt atoms and one CO molecule (see Fig. 1) were extracted every 5 fs. They define a time-resolved trajectory of molecular motion and served as input coordinate files for SSC calculations to simulate time-dependent C 1s XPD patterns for excitation with a photon energy of $h\nu = 1000$ eV, which leads to a kinetic energy of the photoelectrons of 710 eV in vacuum. The single-scattering approximation with spherical wave emission[38] used here is sufficiently accurate for the present case of a single oxygen atom in the forward-scattering geometry.[39]

Since the spatial resolution of the electron detector is on a macroscopic scale, the photoelectron signal is averaged over large parts of the light spot, i.e., the XPD measurement integrates over the forward scattering peaks from an ensemble of molecules. To mimic this, an ensemble averaging over 50 independent simulations was carried out at every time step. Each trajectory started at a different initial point in phase space, randomly sampled from the thermal motion of the field-free system. One should notice that a time-resolved XPD experiment will reveal molecular oscillations only if a large number of molecules undergo a coherent motion.

IV. RESULTS AND DISCUSSION

A. Analysis of a single trajectory

In Fig. 3, the behavior of a single, individual CO molecule bonded at an atop site of a Pt(111) cluster is illustrated over a time interval that ranges from 2.5 ps before to 20 ps after excitation with the THz pulse. In (b) and (c), simulated C 1s XPD patterns covering the 2π solid angle above the surface are shown. In both plots, there is a broad and bright spot associated with the forward scattering peak along the carbon-oxygen direction. Fringes due to first- and higher-order interference between electron waves directly emitted towards the detector and those scattered off the oxygen atom[40] are evident in both cases. In fact, they are all concentric with the peak, but the stereographic projection distorts this relationship while truly mapping them to circles. The position of the main maximum gives the tilting angle θ of the molecule as well as the azimuthal direction ϕ of the tilt very precisely, as can be confirmed by comparison with atomic coordinates of the input cluster. It should be noted that at these high kinetic energies, the backscattering of the photoelectrons off the Pt atoms below the molecule is weak. Therefore, these XPD maps do not show any hint of the three-fold symmetry of the atop binding site. For this very reason, the cluster size for the SSC calculations has been limited to two layers of Pt atoms.

The polar tilt-angle time series of a single molecular trajectory is reported in Fig. 3(a). These data were taken directly from the atomic coordinates of the MD simulation. Polar angles associated with azimuthal angles $90^\circ < \phi < 270^\circ$ were multiplied by a factor of -1, in order to visualize the oscillatory behavior of the wagging motion. The figure shows that even before excitation by the pump pulse (delay $t < 0$ ps), the molecule has a significant wagging motion. This is due to thermal activation of the frustrated translational mode, which is excited with $\bar{n}$ quanta at room temperature,[41,42] where $\bar{n} \approx k_B T/\hbar\omega \approx 3.5$. Although the mean tilting angle should be up to $\theta = 10^\circ$, a single molecule can have larger amplitudes due to statistical fluctuations. When excited by the pump pulse, more energy is transferred into the frustrated

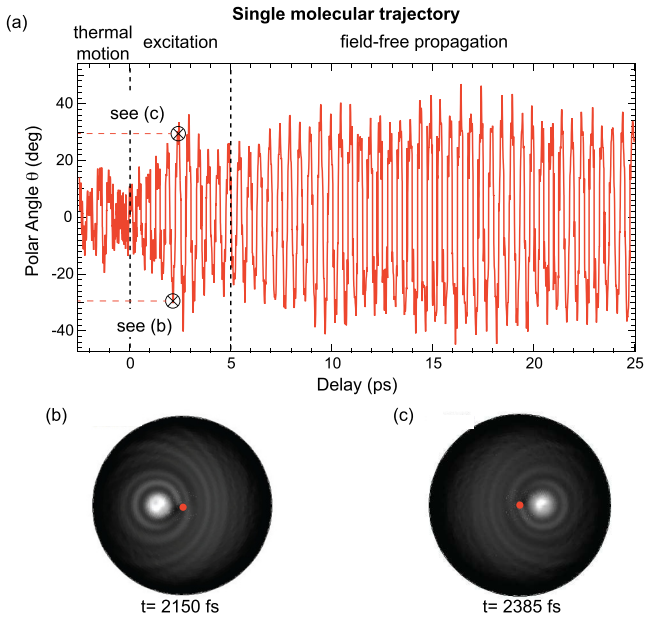

FIG. 3. (a) Time evolution of the wagging motion of a CO molecule on a Pt(111) surface for a single molecule before, during and after excitation with a 2 THz radiation pump pulse. Polar angles of the carbon-to-oxygen direction are plotted, irrespective of the azimuthal direction. For delays between the dashed vertical lines the pump pulse is present. Full XPD maps are displayed in (b) and (c), corresponding to times as marked in (a). The specific delays are chosen to show the near maximum excursions of the polar angle. The two maps are plotted in stereographic projection in a linear grey scale with maximum intensity in white. The red dot indicates emission normal to the surface.

translational mode due to direct coupling to the field and energy transfer from other modes, and the angular amplitude of the wagging motion increases.

After the pump pulse is turned off ($t > 5$ ps), the amplitude does not relax back to its characteristic thermal values within 20 ps even though the slab could serve as a heat reservoir with sufficiently large heat capacity. This is due to the absence in the present model of dissipation via electronic friction induced by the interaction between the vibrating CO-dipole and the electrons of the metal.[43] In the method used here, the only way to dissipate energy into the Pt(111) cluster is by coupling to the lattice vibrations which is very inefficient. Earlier quantum chemical calculations of the lifetime of the wagging mode excited with one quantum ($n = 1$) via only electronic relaxation yielded a value $\tau = 29.4$ ps.[43] In the present work, very high vibrational states are excited by the THz pump pulse ($n > 10$), making a comparison of lifetimes more difficult, but the lifetime of the frustrated translational excitations is clearly overestimated. Nevertheless, the ≈30 ps lifetime found in previous calculations suggests that after excitation the hindered translation remains activated for many vibrational periods which should be sufficient for detection in a real experiment.

In fact, the wagging amplitude shown in Fig. 3(a) increases even further after the THz pulse is gone, and it shows some hints of a beating. Being aware of the absence of electronic friction damping in these calculations, this nevertheless suggests that energy transfer via vibrational coupling between different modes of molecular motion might be observable in such data. Such mode coupling can also be detected in the power spectra of the Pt-C, C-O, and Pt-C-O coordinates and the motion characterizing the frustrated translation. However, such considerations are unable to quantify the coupling strength between the modes. We note in passing that the coupling of the frustrated translation (which is not described by a separate term in the force field) to other degrees of freedom is probably very small as judged from the absence of any relaxation after switching off the external perturbation. This is corroborated further by the observation that the frequency of the frustrated translation before and after excitation is 1.79 THz and 2.08 THz, respectively. In other words, after the perturbation is switched off, the frequency of the frustrated translation does not return to its equilibrium value.

B. Analysis of an ensemble of trajectories

In a real experiment, XPD intensity modulations are averaged over an ensemble of molecules. To mimic this, the 50 diffraction patterns obtained from 50 independent trajectories were averaged at each time step and a molecular movie was created that shows the averaged time-evolution of the full ensemble. In Fig. 4, parts of the movie are presented. It shows the same delay scan covering 27.5 ps as in Fig. 3, where the 5 ps long pump pulse is present from 0 to 5 ps. Before and after this excitation period, the system is unperturbed.

In Fig. 4(a), the time series of average polar tilt angles of the CO molecules is shown. It was determined by extracting the emission maximum of the averaged diffraction maps obtained from the SSC calculations. Before the arrival of the THz pulse, the polar angle is centered around 0°, with much lower fluctuations than in the single trajectory of Fig. 3(a). Although individual molecules show an activated frustrated translational mode, the isotropic distribution of the azimuthal plane of oscillation as well as their incoherent phases leads to an averaging out of the polar tilt angle that is extracted from the averaged XPD maps.

When the linearly polarized pump pulse starts driving the molecular motion, they start to align their azimuthal directions along the light polarization ($\phi = 0°/180°$) and a coherent wagging oscillation begins. This can be understood by the picture of a dipole in an electrical field transversal to the dipole moment: the frustrated rotational frequency of CO on Pt(111) is $\nu = 12.33$ THz.[21] Hence, the rotational movement of a CO molecule is almost one order of magnitude faster than its frustrated translational wagging motion. As a consequence, within a half cycle of the 2 THz pulse during which the electrical field has a constant sign, the molecules have enough time to align their tilting motion parallel to the laser field. Therefore, a coherent oscillation with $\nu = 2$ THz starts for delays $\Delta t > 0$ fs. While the pump pulse is

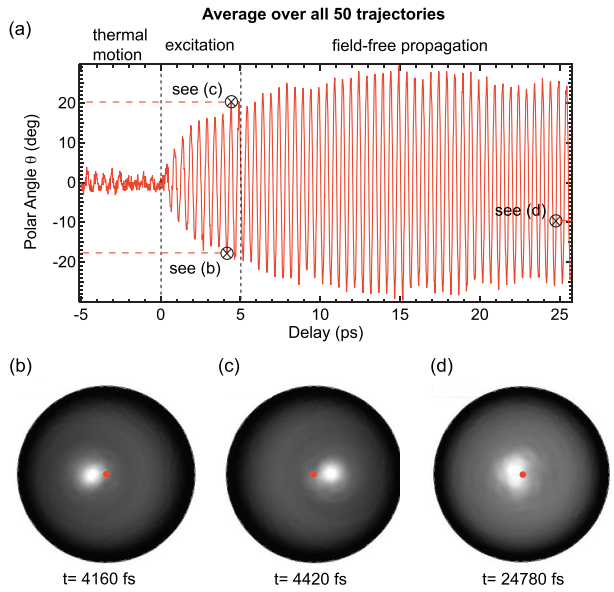

FIG. 4. Simulation of a THz pump-XPD probe measurement. In (a), the time-dependent polar angle of maximum emission from the averaged diffraction maps is plotted. It represents the ensemble-averaged orientation of the CO molecules on Pt(111). For positive delays, an oscillation with $\nu = 2.0$ THz is visible. At delays between the dashed lines the pump pulse is present. (b)–(d) The averaged diffraction maps that were calculated with SSC simulations. No normalization was applied. The delay times of all three patterns are marked in (a) with black circles. Each diffraction map is ensemble averaged over calculations from 50 different cluster files. The red dots in the center of the maps show the normal emission direction.

present, the amplitude of the oscillation increases steadily to approximately $\theta = 20^\circ$ as more and more energy is deposited in the tilting modes of the molecules.

In our model, the absolute magnitudes of the charges on C and O atoms are equal, thus, while the THz field will exert a significant torque on CO, its net force will be zero. Normal mode analysis on the Pt_{7-3}-CO cluster has shown that the frustrated translational and frustrated rotational normal modes can be decomposed into a mixture of translation and rotation of CO in ratios of $90\% : 10\%$ and $7\% : 93\%$, respectively. Thus, both modes involve tilting motion of the molecules which is directly recorded in the XPD data. Furthermore, classically the THz field couples primarily to the higher-frequency frustrated rotations; however, being off-resonant with it will not excite it very effectively. As the frustrated translational mode has also some rotational character, it can be excited by a near-resonant oscillating torque exerted by the THz field. In the ensemble averaged evolution of the polar angle (see Fig. 4), it is observed that after switching off the THz field, the amplitude of the oscillations in the polar angle keeps increasing for a while. This can be explained by considering an energy flow from the highly excited frustrated translational mode to the less excited frustrated rotational mode. The amplitude reaches a maximum about 10 ps after the THz pulse has gone, which suggests that the two modes equilibrate. In a real experiment, the observed increase would be counteracted by a relaxation due to electronic excitations within the metal surface. Nevertheless, these data suggest that one should be able to extract information about the temporal evolution of the energy transfer between different modes from such experiments.

Figures 4(b)–4(d) show individual frames from the molecular movie created from the averaged diffraction maps. Due to the coherent molecular motion, distinct forward scattering maxima are visible for each case, also at times of maximum negative (b) and positive (c) excursion within the wagging mode. On the other hand, the interference fringes that are visible in the frames from the single trajectory (Figs. 3(b) and 3(c)) are here completely smeared out due to the averaging. As shown in Fig. 4(d), the forward scattering peak is broadened at a later time, 20 ps after the THz pulse, because the azimuthal alignment of the molecules in the THz field has relaxed and the wagging motion becomes more isotropic.

Fig. 5 illustrates this broadening more clearly, along with the disappearance of the interference fringes, by displaying polar sections along the x direction through the simulated diffraction maps. More importantly, the curves demonstrate that the diffraction contrast remains quite pronounced even after the ensemble averaging. The contrast can be quantified by the anisotropy of the forward scattering peak, defined as $A = (I_{max} - I_{ped})/I_{max}$, where I_{max} is the maximum intensity of the peak and I_{ped} is a mean value of the pedestal intensity to the left and right of the peak. While single trajectories (Fig. 5(a)) show values of typically about $A = 0.7$, ensemble averaging (Fig. 5(b)) reduces these values to about 0.63 near the end of the THz pulse, and finally to about 0.5 after the relaxation of the azimuthal alignment of the molecules.

The temporal evolution of the azimuthal alignment is illustrated in Fig. 6, in which the polar and azimuthal positions of the oxygen atoms with respect to the carbon emitters are plotted for three different times before, during, and after the THz pulse. While the distribution of the 50 different molecular trajectories at delay $\Delta t = -1125$ fs shows no preferred azimuthal alignment, the molecules have the highest azimuthal order at the end of the pump period, to which $\Delta t = 4150$ fs is close. At times long after the pump pulse, like at $\Delta t = 24960$ fs, the molecule orientations spread over a larger azimuthal range, which is also seen in the longer delay data of Fig. 4(d). The two delays, $\Delta t = 4150$ and $\Delta t = 24960$ fs, were selected such that the coherent wagging oscillation is at maximum amplitude.

V. CONCLUSIONS AND OUTLOOK

The present simulations show how time-resolved XPD can visualize structural dynamics, taking advantage of coherent motion in an ensemble of adsorbed molecules. An example of a molecular movie is presented in which molecular motion can be followed in real time and with atomic resolution. In a realistic experiment, e.g., at an XFEL, the x-ray pulses should have a temporal width of the order of a few tens of femtoseconds in order to achieve a reasonable sampling of the 1.79 THz oscillation. A coverage of $\Theta = 1/6$ should not be exceeded because of the different adsorption regimes and accordingly opposite dipole orientations of the molecules. Antiphase oscillations at atop and bridge adsorption sites would lead to a blurring of the resulting time-dependent XPD patterns.

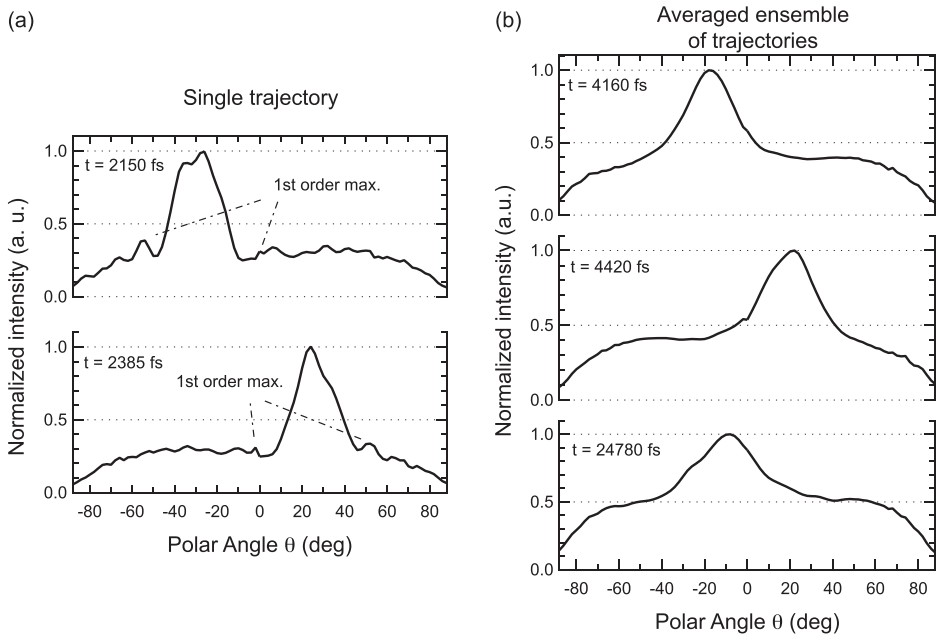

FIG. 5. Polar intensity scans for quantifying the angular contrast. (a) and (b) Sections along the x direction through the simulated photoelectron diffraction maps displayed in Figs. 3 and 4, respectively. All curves have been normalized so that maximum intensity equals unity.

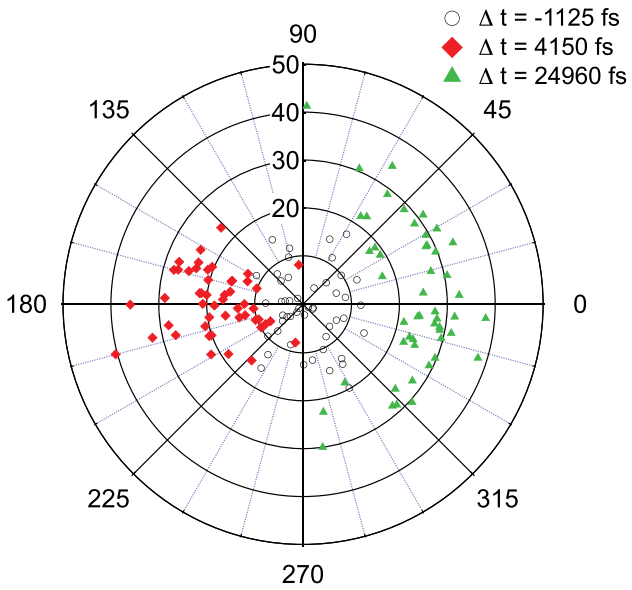

FIG. 6. Angular order of the CO molecules. At three different times, the angular position (θ, ϕ) of the oxygen atom with respect to the carbon emitter is plotted for each of the 50 trajectories: before the THz pulse (black), near the end of the pulse (red) and 20 ps after the pulse (green).

While THz pulses with a shape as used in these toy-model simulations can be synthesized, in principle, the currently most common half-cycle THz pulses should also be able to coherently excite the wagging mode discussed here. Interaction of the THz field with the underlying metal surface is an issue. The polarization parallel to the surface required for this experiment will be very effectively screened, leading to a node exactly where the high field strength is needed. In order to overcome this problem, one will have to fabricate surfaces with small, crystallographically aligned Pt(111) islands on a dielectric substrate that could lead to THz field enhancement at the metallic surfaces via plasmonic effects.[44]

The THz fluence will have to be carefully adjusted for maximum excitation of wagging motion without excessive desorption of CO molecules. For excitation with IR photons, the CO desorption rate depends on both, the pulse duration and fluence. It was shown that desorption is negligible for pulse durations longer than 500 fs,[45] but only up to a fluence of $F = 5$ mJ/cm^2. In the MD simulations, a field amplitude of $E = 6 \times 10^8$ V/m was used in order to obtain these strong coherent wagging motions. With a pulse duration of $t = 5$ ps, a comparably large fluence of $F = 239$ mJ/cm^2 results. Since the metal-adsorbate stretch modes are much faster than the THz oscillations,[21] coupling to these modes, which are the main responsible vibrational modes for desorption, will be weak, in particular, for the chosen polarization of the THz pulse. Moreover, the results of our work suggest that the oscillatory signal in the XPD data could still be picked up with THz fields reduced by an order of magnitude. And in any case the THz and x-ray beams will be scanned across the surface as is usual for XFEL experiments on solid samples.

A further discussion of desorption mechanisms and the limits of field strength is beyond the scope of this work. The same applies to the ability of the substrate to screen the electric field and thus to influence the coupling of the THz radiation to the wagging motion of CO. Moreover, electronic relaxation processes leading to the faster attenuation of the coherent motion have not been included in this work. Introducing electronic friction[46] in the MD simulations would make the computational model more realistic. Finally, the photoelectrons will be subject to strong streaking by the THz field while it is present,[47] but the structural dynamics after the excitation should be free from measurement artifacts.

In summary, this study demonstrates that time-resolved XPD is a promising technique for following the structural dynamics of small molecules adsorbed on a surface with femtosecond

resolution. Importantly, the ensemble averaging, which is inherent in this technique, does not smear out the structural information as long as vibrational modes are excited coherently. THz radiation is well suited for this purpose. The amount of structural detail in ensemble averaged data is high enough that energy transfer between different modes might potentially be observed.

A full digital version of the two molecular movies, i.e., single trajectory (Fig. 3) and ensemble averaged data (Fig. 4), can be downloaded in the supplementary material.[48]

ACKNOWLEDGMENTS

Financial support from the Swiss National Science Foundation through the NCCR MUST and from Project No. 200021-117810 (to M.M.) is gratefully acknowledged.

[1]A. H. Zewail, "Femtochemistry: Atomic-scale dynamics of the chemical bond," J. Phys. Chem. A **104**, 5660 (2000).
[2]H. Ihee, V. A. Lobastov, U. M. Gomez, B. M. Goodson, R. Srinivasan, C.-Y. Ruan, and A. H. Zewail, "Direct imaging of transient molecular structures with ultrafast diffraction," Science **291**, 458–462 (2001).
[3]J. Kuepper, S. Stern, L. Holmegaard, F. Filsinger, A. Rouzee, A. Rudenko, P. Johnsson, A. V. Martin, M. Adolph, A. Aquila, S. Bajt, A. Barty, C. Bostedt, J. Bozek, C. Caleman, R. Coffee, N. Coppola, T. Delmas, S. Epp, B. Erk, L. Foucar, T. Gorkhover, L. Gumprecht, A. Hartmann, R. Hartmann, G. Hauser, P. Holl, A. Hoemke, N. Kimmel, F. Krasniqi, K.-U. Kuehnel, J. Maurer, M. Messerschmidt, R. Moshammer, C. Reich, B. Rudek, R. Santra, I. Schlichting, C. Schmidt, S. Schorb, J. Schulz, H. Soltau, J. C. H. Spence, D. Starodub, L. Strueder, J. Thogersen, M. J. J. Vrakking, G. Weidenspointner, T. A. White, C. Wunderer, G. Meijer, J. Ullrich, H. Stapelfeldt, D. Rolles, and H. N. Chapman, "X-ray diffraction from isolated and strongly aligned gas-phase molecules with a free-electron laser," Phys. Rev. Lett. **112**, 083002 (2014).
[4]J. Norskov, T. Bligaard, A. Logadottir, S. Bahn, L. Hansen, M. Bollinger, H. Bengaard, B. Hammer, Z. Sljivancanin, M. Mavrikakis, Y. Xu, S. Dahl, and C. Jacobsen, "Universality in heterogeneous catalysis," J. Catal. **209**, 275–278 (2002).
[5]F. Besenbacher, I. Chorkendorff, B. Clausen, B. Hammer, A. Molenbroek, J. Norskov, and I. Stensgaard, "Design of a surface alloy catalyst for steam reforming," Science **279**, 1913–1915 (1998).
[6]M. Bonn, C. Hess, S. Funk, J. H. Miners, B. N. J. Persson, M. Wolf, and G. Ertl, "Femtosecond surface vibrational spectroscopy of CO adsorbed on Ru(001) during desorption," Phys. Rev. Lett. **84**, 4653–4656 (2000).
[7]H. Petek, M. J. Weida, H. Nagano, and S. Ogawa, "Real-time observation of adsorbate atom motion above a metal surface," Science **288**, 1402–1404 (2000).
[8]H. Petek and S. Ogawa, "Surface femtochemistry: Observation and quantum control of frustrated desorption of alkali atoms from noble metals," Annu. Rev. Phys. Chem. **53**, 507–531 (2002).
[9]M. Dell'Angela, T. Anniyev, M. Beye, R. Coffee, A. Föhlisch, J. Gladh, T. Katayama, S. Kaya, O. Krupin, J. LaRue, A. Mogelhoj, D. Nordlund, J. K. Norskov, H. Öberg, H. Ogasawara, H. Öström, L. G. M. Pettersson, W. F. Schlotter, J. A. Sellberg, F. Sorgenfrei, J. J. Turner, M. Wolf, W. Wurth, and A. Nilsson, "Real-time observation of surface bond breaking with an x-ray laser," Science **339**, 1302–1305 (2013).
[10]H. Öström, H. Öberg, H. Xin, J. LaRue, M. Beye, M. Dell'Angela, J. Gladh, M. L. Ng, J. A. Sellberg, S. Kaya, G. Mercurio, D. Nordlung, M. Hantschmann, F. Hieke, D. Kühn, W. F. Schlotter, G. L. Dakovski, J. J. Turner, M. P. Minitti, A. Mitra, S. P. Moeller, A. Föhlisch, M. Wolf, W. Wurth, M. Persson, J. K. Norskov, F. Abild-Pedersen, H. Ogasawara, L. G. M. Pettersson, and A. Nilsson, "Probing the transition state region in catalytic CO oxidation on Ru," Science **347**, 978–982 (2015).
[11]C. Ruan, F. Vigliotti, V. Lobastov, S. Chen, and A. Zewail, "Ultrafast electron crystallography: Transient structures of molecules, surfaces, and phase transitions," Proc. Natl. Acad. Sci. U.S.A. **101**, 1123–1128 (2004).
[12]R. Locher, L. Castiglioni, M. Lucchini, M. Greif, L. Gallmann, J. Osterwalder, M. Hengsberger, and U. Keller, "Energy-dependent photoemission delays from noble metal surfaces by attosecond interferometry," Optica **2**, 405–410 (2015).
[13]J. Osterwalder, "Structural effects in XPS and AES: Diffraction," in *Surface Analysis by Auger and X-Ray Photoelectron Spectroscopy*, edited by D. Briggs and J. Grant (IM Publications and Surface Spectra Limited, 2003), p. 557.
[14]Y. Matsumoto and K. Watanabe, "Coherent vibrations of adsorbates induced by femtosecond laser excitation," Chem. Rev. **106**, 4234–4260 (2006).
[15]B. D. Patterson, J. Sa, A. Ichsanow, C. P. Hauri, C. Vicario, C. Ruchert, I. Czekaj, R. Gehrig, H. C. Sigg, J. A. van Bokhoven, B. Pedrini, and R. Abela, "Can energetic terahertz pulses initiate surface catalytic reactions on the picosecond time scale?," Chim. Int. J. Chem. **65**, 323–325 (2011).
[16]I. Langmuir, "The mechanism of the catalytic action of platinum in the reactions $2CO + O_2 = 2CO_2$ and $2H_2 + O_2 = 2H_2O$," Trans. Faraday Soc. **17**, 621 (1922).
[17]Y. Y. Yeo, L. Vattuone, and D. A. King, "Calorimetric heats for CO and oxygen adsorption and for the catalytic CO oxidation reaction on Pt(111)," J. Chem. Phys. **106**, 392 (1997).
[18]J. Wintterlin, S. Volkening, T. Janssens, T. Zambelli, and G. Ertl, "Atomic and macroscopic reaction rates of a surface-catalyzed reaction," Science **278**, 1931–1934 (1997).
[19]G. Ertl, M. Neumann, and K. Streit, "Chemisorption of CO on the Pt(111) surface," Surf. Sci. **64**, 393–410 (1977).
[20]H. Steininger, S. Lehwald, and H. Ibach, "On the adsorption of CO on Pt(111)," Surf. Sci. **123**, 264–282 (1982).
[21]A. P. Graham, "The low-frequency vibrational modes of c(4 × 2) CO on Pt(111)," J. Chem. Phys. **109**, 9583 (1998).
[22]D. F. Ogletree, M. A. V. Hove, and G. A. Somorjai, "LEED intensity analysis of the structures of clean Pt(111) and of CO adsorbed on Pt(111) in the c(4 × 2) arrangement," Surf. Sci. **173**, 351 (1986).
[23]P. Deshlahra, J. Conway, E. E. Wolf, and W. F. Schneider, "Influence of dipole–dipole interactions on coverage-dependent adsorption: CO and NO on Pt(111)," Langmuir **28**, 8408–8417 (2012).
[24]H. Ueba, "Chemical effects on vibrational properties of adsorbed molecules on metal surfaces: Coverage dependence," Surf. Sci. **188**, 421–455 (1987).

[25]G. Blyholder, "Molecular orbital view of chemisorbed carbon monoxide," J. Phys. Chem. **68**, 2772 (1964).
[26]A. Nilsson and L. G. M. Pettersson, "Chemical bonding on metal surfaces," in *Model Systems in Catalysis: Single Crystals to Supported Enzyme Mimics*, edited by R. M. Rioux (Springer Verlag, New York, 2010), pp. 253–273.
[27]D. A. Wesner, U. Breuer, O. Knauff, and H. P. Bonzel, "XPD studies of adsorbates and surface melting," Phys. Scr. **1990**(T31), 247–254.
[28]A. Lahee, J. Toennies, and C. Wöll, "Low energy adsorbate vibrational modes observed with inelastic helium atom scattering: CO on Pt(111)," Surf. Sci. **177**, 371–388 (1986).
[29]M. P. Allen and D. J. Tildesley, *Computer Simulation of Liquids* (Oxford University Press, Oxford, 1991).
[30]B. R. Brooks, R. E. Bruccoleri, B. D. Olafson, D. J. States, S. Swaminathan, and M. Karplus, "CHARMM: A program for macromolecular energy, minimization, and dynamics calculations," J. Comput. Chem. **4**, 187–217 (1983).
[31]B. R. Brooks, C. L. Brooks, A. D. Mackerell, L. Nilsson, R. J. Petrella, B. Roux, Y. Won, G. Archontis, C. Bartels, S. Boresch, A. Caflisch, L. Caves, Q. Cui, A. R. Dinner, M. Feig, S. Fischer, J. Gao, M. Hodoscek, W. Im, K. Kuczera, T. Lazaridis, J. Ma, V. Ovchinnikov, E. Paci, R. W. Pastor, C. B. Post, J. Z. Pu, M. Schaefer, B. Tidor, R. M. Venable, H. L. Woodcock, X. Wu, W. Yang, D. M. York, and M. Karplus, "CHARMM: The biomolecular simulation program," J. Comput. Chem. **30**, 1545–1614 (2009).
[32]H. Heinz, R. A. Vaia, B. L. Farmer, and R. R. Naik, "Accurate simulation of surfaces and interfaces of face-centered cubic metals using 12-6 and 9-6 Lennard-Jones potentials," J. Phys. Chem. C **112**, 17281–17290 (2008).
[33]M. J. Frisch, G. W. Trucks, H. B. Schlegel, G. E. Scuseria, M. A. Robb, J. R. Cheeseman, G. Scalmani, V. Barone, B. Mennucci, G. A. Petersson, H. B. Nakatsuji, M. Caricato, X. Li, H. P. Hratchian, A. F. Izmaylov, J. Bloino, G. Zheng, J. L. Sonnenberg, M. Hada, M. Ehara, K. Toyota, R. Fukuda, J. Hasegawa, M. Ishida, T. Nakajima, Y. Honda, O. Kitao, H. Nakai, T. Vreven, J. A. Montgomery, Jr., J. E. Peralta, F. Ogliaro, M. Bearpark, J. J. Heyd, E. Brothers, K. N. Kudin, V. N. Staroverov, R. Kobayashi, J. Normand, K. Raghavachari, A. Rendell, J. C. Burant, S. S. Iyengar, J. Tomasi, M. Cossi, N. Rega, J. M. Millam, M. Klene, J. E. Knox, J. B. Cross, V. Bakken, C. Adamo, J. Jaramillo, R. Gomperts, R. E. Stratmann, O. Yazyev, A. J. Austin, R. Cammi, C. Pomelli, J. W. Ochterski, R. L. Martin, K. Morokuma, V. G. Zakrzewski, G. A. Voth, P. Salvador, J. J. Dannenberg, S. Dapprich, A. D. Daniels, Ö. Farkas, J. B. Foresman, J. V. Ortiz, J. Cioslowski, and D. J. Fox, Gaussian-09, Revision D.01, Gaussian Inc., Wallingford, CT, 2009.
[34]A. D. Boese and J. M. L. Martin, "Development of density functionals for thermochemical kinetics," J. Chem. Phys. **121**, 3405–3416 (2004).
[35]Y.-W. Huang and S.-L. Lee, "Hybrid DFT and hyper-GGA DFT studies of the CO adsorption on Pt nanoclusters: Effects of the cluster size and better CO LUMO description," Chem. Phys. Lett. **492**, 98–102 (2010).
[36]R. S. Mulliken, "Electronic population analysis on LCAO–MO molecular wave functions I," J. Chem. Phys. **23**, 1833–1840 (1955).
[37]NIST Computational Chemistry Comparison and Benchmark Database, NIST Standard Reference Database Number 101, Release 16a, August 2013, edited by Russell D. Johnson III, http://cccbdb.nist.gov/.
[38]D. J. Friedman and F. C. S, "Final-state effects in photoelectron diffraction," J. Electron Spectrosc. Relat. Phenom. **51**, 689–700 (1990).
[39]H. Aebischer, T. Greber, J. Osterwalder, A. Kaduwela, D. Friedman, G. Herman, and C. Fadley, "Material dependence of multiple-scattering effects associated with photoelectron and auger electron diffraction along atomic chains," Surf. Sci. **239**, 261–264 (1990).
[40]T. Greber, J. Wider, E. Wetli, and J. Osterwalder, "X-ray photoelectron diffraction in the backscattering geometry: A key to adsorption sites and bond lengths at surfaces," Phys. Rev. Lett. **81**, 1654–1657 (1998).
[41]E. Schweizer, B. N. J. Persson, M. Tüshaus, D. Hoge, and A. M. Bradshaw, "The potential energy surface, vibrational phase relaxation and the order-disorder transition in the adsorption system Pt(111)-CO," Surf. Sci. **213**, 49–89 (1989).
[42]H. Over, W. Moritz, and G. Ertl, "Anisotropic atomic motions in structural-analysis by low-energy electron-diffraction," Phys. Rev. Lett. **70**, 315–318 (1993).
[43]V. Krishna and J. C. Tully, "Vibrational lifetimes of molecular adsorbates on metal surfaces," J. Chem. Phys. **125**, 054706 (2006).
[44]G. Herink, C. Wimmer, and C. Ropers, "Field emission at terahertz frequencies: AC-tunneling and ultrafast carrier dynamics," New J. Phys. **16**, 123005 (2014).
[45]L. Cai, X. D. Xiao, and M. Loy, "Femtosecond laser desorption of CO from the Pt(111) surface," Surf. Sci. **464**, L727–L731 (2000).
[46]M. Head-Gordon and J. C. Tully, "Molecular dynamics with electronic frictions," J. Chem. Phys. **103**, 10137 (1995).
[47]L. Castiglioni, D. Leuenberger, M. Greif, and M. Hengsberger, "Attosecond transversal streaking to probe electron dynamics at surfaces," in *Multiphoton Processes and Attosecond Physics*, Springer Proceedings in Physics Vol. 125, edited by K. Yamanouchi and K. Midorikawa (Springer, Berlin, Heidelberg), 2012), p. 365.
[48]See supplementary material at http://dx.doi.org/10.1063/1.4922611 for full digital versions of the two molecular movies.